STING Agonist-Based Treatment Promotes Vascular Normalization and Tertiary Lymphoid Structure Formation in the Therapeutic Melanoma Microenvironment

Supplementary Figures

Manoj Chelvanambi[1], Ronald J. Fecek[2], Jennifer L. Taylor[2], Walter J. Storkus[1-5*]

[1] Department of Immunology, University of Pittsburgh School of Medicine (UPSOM), Pittsburgh PA 15213

[2] Department of Dermatology (UPSOM), Pittsburgh PA 15213

[3] Department of Pathology (UPSOM), Pittsburgh PA 15213

[4] Department of Bioengineering (UPSOM), Pittsburgh PA 15213

[5] University of Pittsburgh Cancer Institute, Pittsburgh PA 15213

Fig. S1:

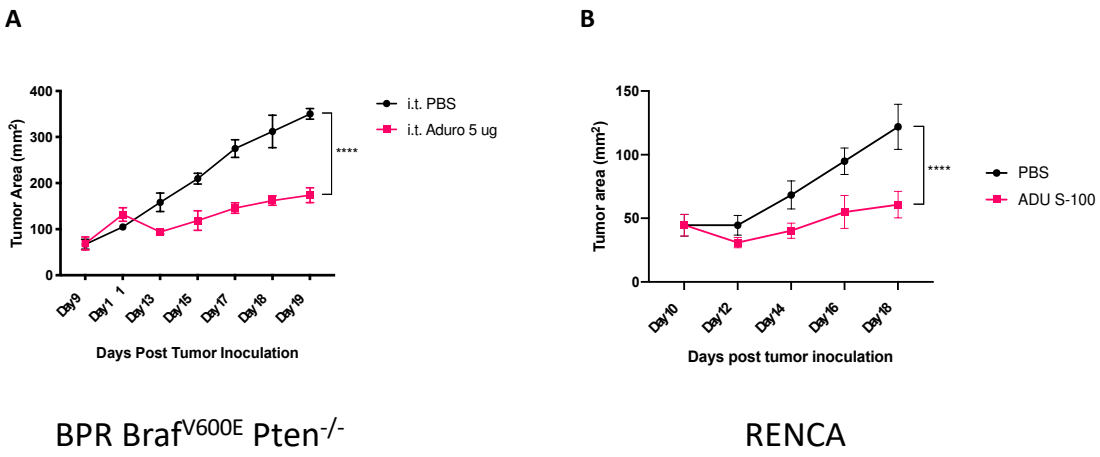

Figure S1: STING agonist ADU S-100 slows growth of BPR Melanoma and RENCA renal cell carcinomas in syngeneic immunocompetent hosts. Representative tumor growth curves from treated cohorts (n = 5/group) of C57BL/6 mice bearing established BPR melanomas (**A**) or BALB/c mice bearing established RENCA renal cell carcinomas (**B**) as described in **Fig. 1** and Materials and Methods. Note significantly slower tumor growth kinetics when mice were treated with STING agonist ADU S-100 intratumorally. Tumors were measured using calipers and sizes are represented as total tumor area (calculated as small axis x large axis). ****p < 0.0001, Two-Way ANOVA. Representative tumor growth curves from three independent experiments.

Fig. S2:

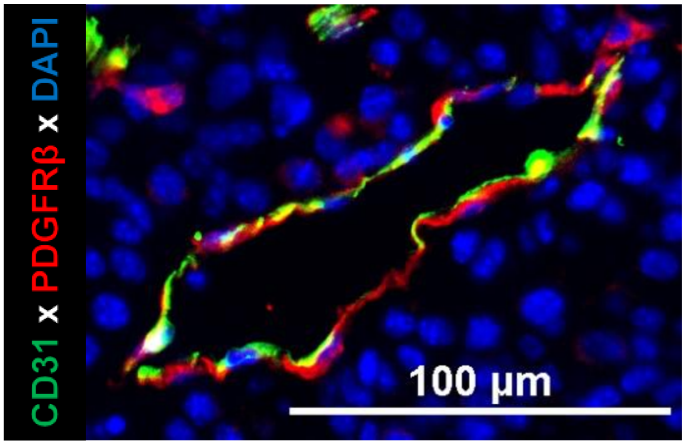

Figure S2: Representative high-magnification immunofluorescence image demonstrating separate spatial stacking of PDGFRβ⁺ pericytes and CD31⁺ VEC in normalized blood vessels found in B16 melanomas treated with i.t. ADU S-100 (as described in **Fig. 2**). Note yellow (overlap of red/green signals) pseudo-coloring of the abluminal VEC cell surfaces with tightly approximated pericyte cell surfaces. Scale bar = 100µm

Fig. S3:

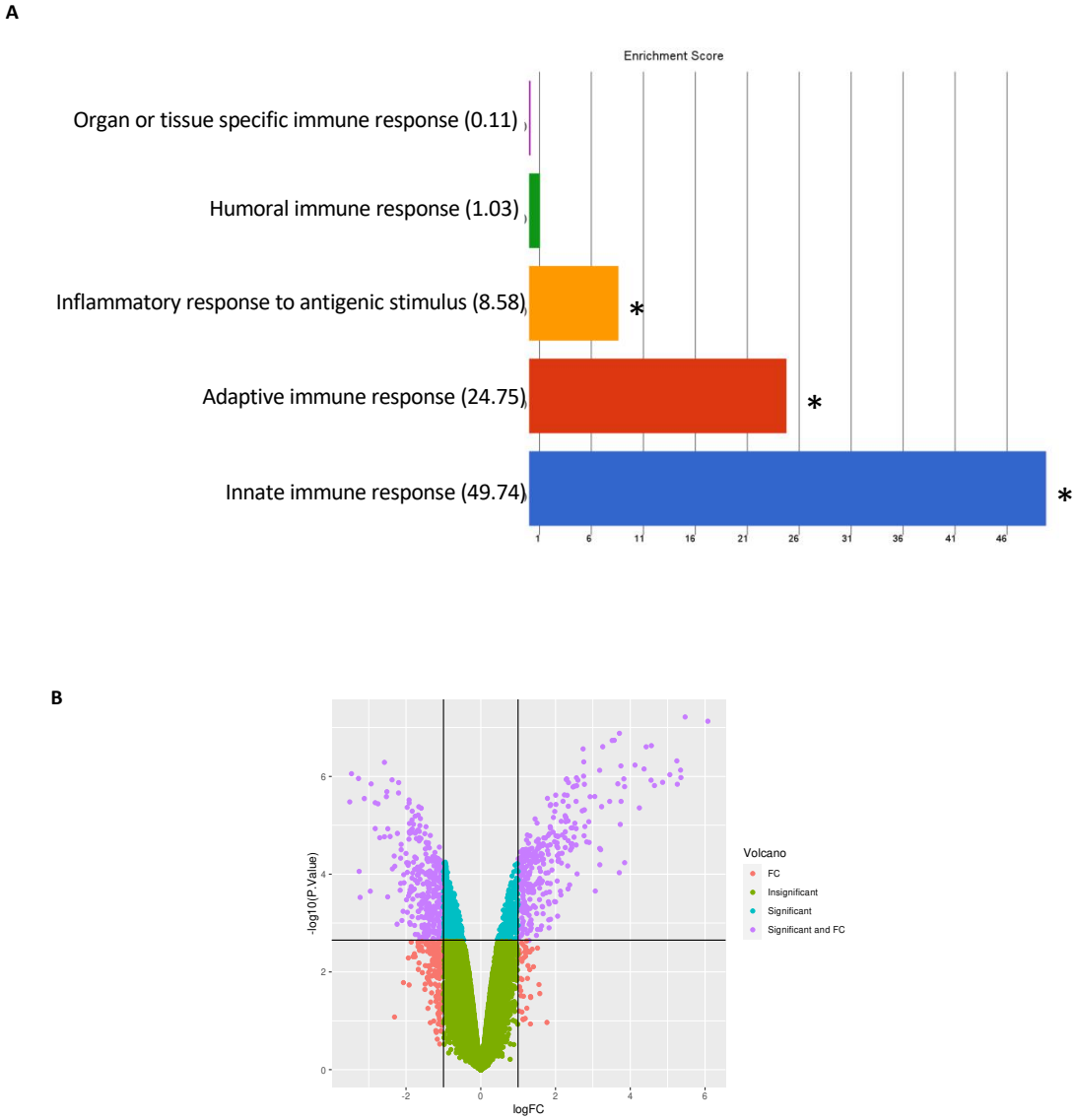

Figure S3: Transcriptional profiling and pathway analysis of CD11c⁺ DC treated with ADU S-100 vs control media. A. Biological processes associated with top GO term, immune response (GO:0006955), enriched in ADU S-100-treated CD11c⁺ DCs. *p-value < 0.05, One-way ANOVA. **B**. Volcano plot of CD11c⁺ DC genes analyzed via microarray. ~1300 genes (shown in purple) were found to be differentially expressed (|log2FC|>1 & adjusted p-value < 0.05) and were used for pathway and GO enrichment.

Fig. S4:

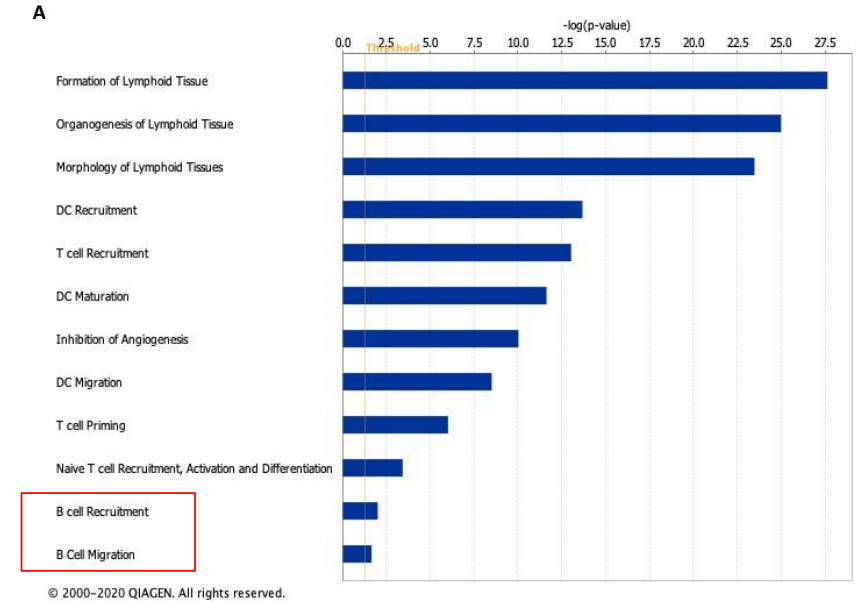

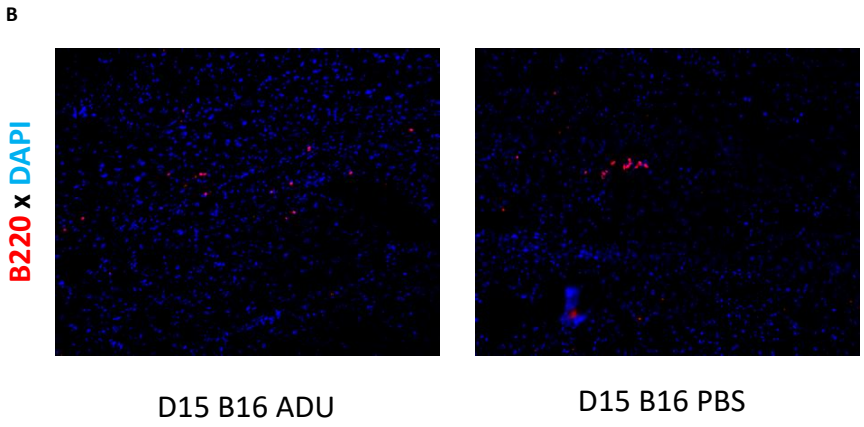

Figure S4: STING activation does not improve B220+ B cell recruitment to s.c. B16.F10 melanomas. A. Gene-set enrichment of STING activated CD11c^{+} DC gene expression showing significant TLS nucleating, DC recruiting and T cell recruiting signatures, but poor B cell recruiting signatures. Threshold = -log(p-value) of 1.3 or p-value of 0.05. **B**. Representative immunofluorescence image showing no observable differences in B cell infiltration with ADU S-100 vs. PBS treatment of B16.F10 melanomas *in vivo*.

Fig. S5

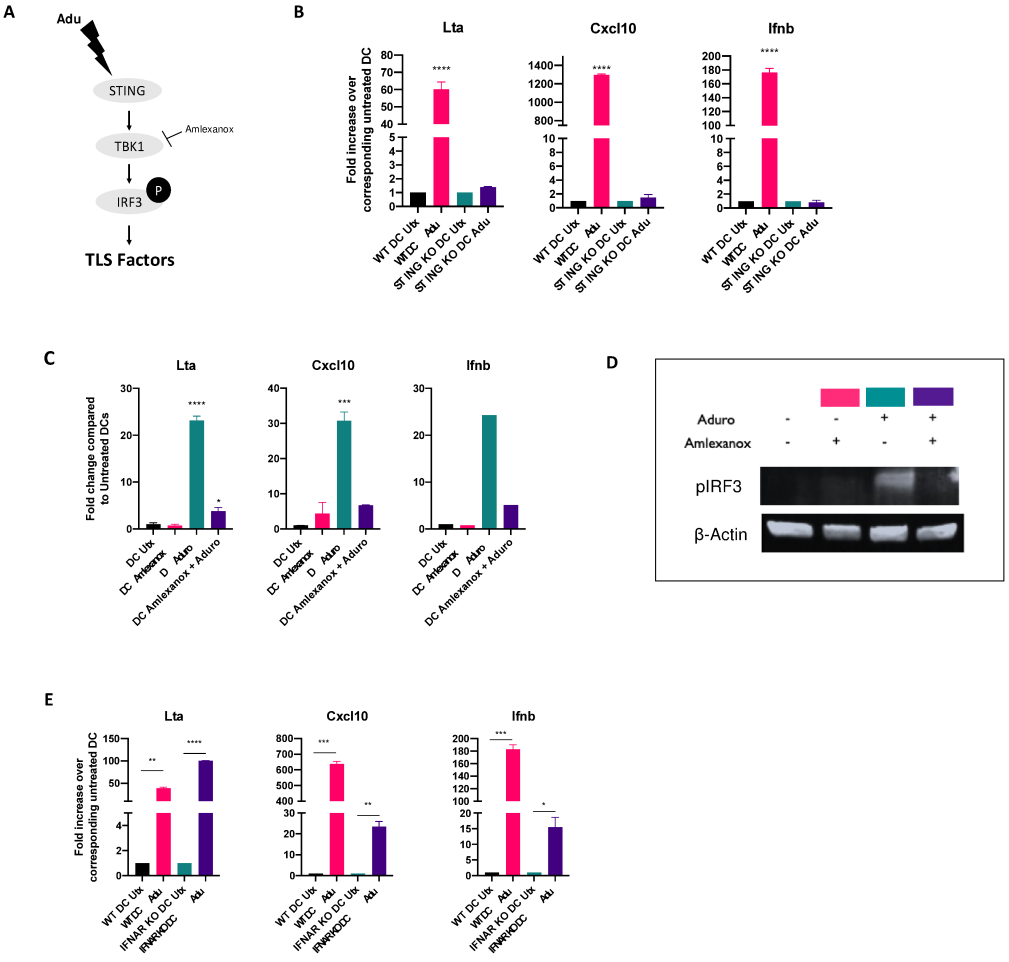

Figure S5: STINGactivation issufficient to promote production of TLS factors through a STING-TBK1-IRF3 signaling cascade. A. Schematic representing canonical STING signaling cascade involving TBK1 and IRF3. **B**. STING activation significantly increases transcript levels of TLS factors in CD11c⁺ DCs from WT hosts which is absent in DCs from STING KO hosts. ****p < 0.0001, One-Way ANOVA. **C**. Inhibition of TBK1 using Amlexanox prior to STING activation ablates production of STING associated TLS factors. *p < 0.05, ***p < 0.0002, ****p < 0.0001, One-Way ANOVA. **D**. Immunoblotting confirms upregulation of TLS associated transcripts in CD11c⁺ DCs (in panel **C**) occurs only with IRF3 activation/phosphorylation (S396). **E.** IFNAR KO DC retain ability to produce TLS factors upon STING activation. *p < 0.05, **p < 0.002, ***p < 0.0002, ****p < 0.0001, unpaired t-test.

Fig. S6:

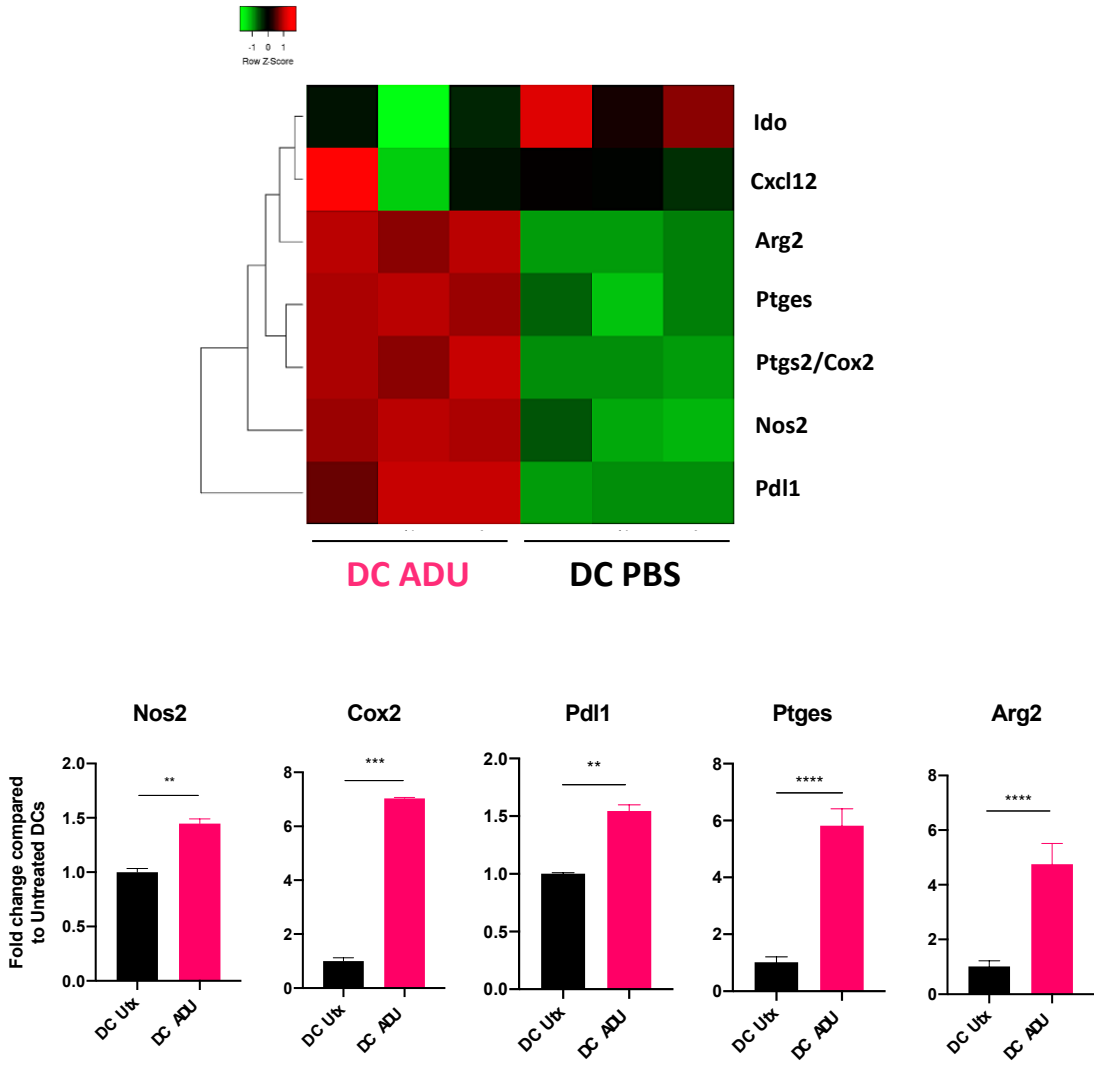

Figure S6: STING mediated inflammation concomitantly upregulates expression of immune regulatory molecules by CD11c⁺ DC. A. Transcriptional profiling of isolated CD11c⁺ DC treated with ADU S-100 vs. control media for immunoregulatory gene products including Arg2, Nos2, Pdl1, Ptges and Ptgs2/COX-2. Specific transcript levels determined by qRT-PCR as in **Fig. 3**. **p < 0.002, ***p < 0.0002, ****p < 0.0001, unpaired t-test.

Fig. S7:

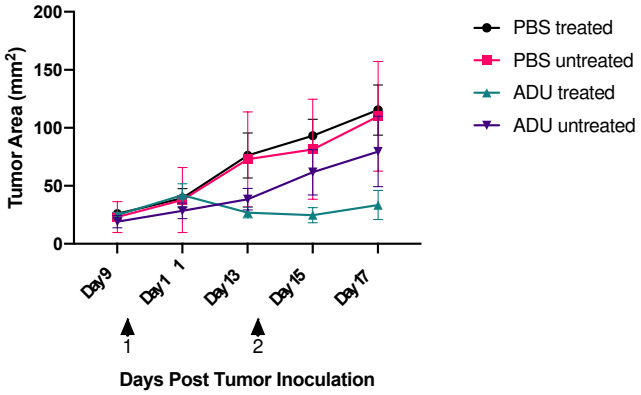

Figure S7: Lack of prolonged systemic response with ADU S-100 in bilateral B16.F10 models. B16.F10 tumor growth curves from pilot trials showing lack of extended therapy in un-injected left flank tumors of mice receiving 5 μg ADU S-100 (i.t.) in right-flank tumors.

Table S1:

Antigen	Clone	Vendor	Concentration
CD3 Alexa Fluor 647	17A2	BioLegend	1:50
CD45 Alexa Fluor 488	30-F-11	BioLegend	1:100
CD11c Alexa Fluor 488	N418	BioLegend	1:100
PNAd Purified	MECA 79	BD Pharmingen	1:100
CD31 Alexa Fluor 647	MEC 13.3	BioLegend	1:50
B220 FITC	RA3-6B2	Pharmingen	1:100
Lyve-1 Purified	ALY7	Invitrogen	1:100
PRGFRβ PE	APB5	Invitrogen	1:100
VCAM1 Purified	AF643	R&D Systems	1:100
Lectin Alexa Fluor 488	DL-1174	Vector Labs	200 µg/mouse
CD133	N/A	Santa Cruz Bio	1:100
Jarid1b	N/A	Abcam	1:500
pIRF3	CST 29047S	CST	1:1000
β-Actin	ab6276	Abcam	1:10000

Supplemental Table 1: List of antibodies and corresponding concentrations used for immunoblotting and immunofluorescence experiments

Table S2:

Target	Forward Primer	Reverse Primer
Ifnb	TGGGAGATGTCCTCAACTGC	CCAGGCGTAGCTGTTGTACT
Lta	GCCCATCCACTCCCTCAGAA	TGCTGGGGTACCCAACAAGG
Ltb	GGACGTCGGGTTGAGAAGAT	ACGGTTTGCTGTCATCCAGT
Cxcl10	ATGACGGGCCAGTGAGAATG	TCGTGGCAATGATCTCAACAC
Ptgs2/Cox2	GGGCCCTTCCTCCCGTAGA	TGAGCCTTGGGGGTCAGGGA
Nos2	TCCTGGACATTACGACCCCT	CTCTGAGGGCTGACACAAGG
Pdl1	TCACTTGCTACGGGCGTTTA	ATCGTGACGTTGCTGCCATA
Ccl19	CCTGGGAACATCGTGAAAGC	TAGTGTGGTGAACACAACAGC
Ccl21	GTGATGGAGGGGGTCAGGA	GGGATGGGACAGCCTAAACT
Cxcl13	TCTCCAGGCCACGGTATTCT	GGGGCGTAACTTGAATCCGA
Tnfsf15	GACTGTATGCTTCGGGCCAT	ATTGTCAGGTGTGCTCTCGG
Arg2	ATCGGCTGATTGGCAAAAGG	AATCCCCCTACAACAGGGGT
Ptges	GCTGCGGAAGAAGGCTTTTG	GCTCCACATCTGGGTCACTC

Supplemental Table 2: List of gene targets and corresponding primer sequences used for quantitative real-time PCR analyses